Mineralogy and Petrology (2006) 87: 143–162
DOI 10.1007/s00710-006-0120-1

Mineralogy and Petrology
Printed in Austria

A record of pre-Variscan Barrovian regional metamorphism in the eastern part of the Slavonian Mountains (NE Croatia)

D. Balen[1], **P. Horváth**[2], **B. Tomljenović**[3], **F. Finger**[4], **B. Humer**[4], **J. Pamić**[†,5], and **P. Árkai**[2]

[1] Faculty of Science, University of Zagreb, Zagreb, Croatia
[2] Institute for Geochemical Research, Hungarian Academy of Sciences, Budapest, Hungary
[3] Faculty of Mining, Geology & Petroleum Engineering, University of Zagreb, Zagreb, Croatia
[4] University of Salzburg, Salzburg, Austria
[5] Croatian Academy of Sciences and Arts, Zagreb, Croatia

Received March 31, 2005; revised version accepted January 16, 2006
Published online April 20, 2006;
Editorial handling: K. Stüwe

Summary

Petrological investigations and monazite dating are carried out on medium-grade metamorphic rocks (micaschist, gneiss and amphibolite) from the Kutjevačka Rijeka transect in the Slavonian Mts., Tisia Unit (NE Croatia). Field, mesoscopic and microstructural observations, as well as the preserved mineral chemistry, point to a single metamorphic event during peak assemblage growth reaching amphibolite facies conditions of ca. 600–650 °C and 8–11 kbar. Th, U and Pb contents of yttrium-rich accessory monazites indicate a pre-Variscan, i.e. Ordovician-Silurian age (444 ± 19 and 428 ± 25 Ma) for the medium-grade metamorphism of garnet-bearing micaschist.

Introduction

The crystalline rocks from the southern part of the Tisia Unit (Slavonian Mountains in Croatia) are some of the least known basement outcrops in the Variscan belt. Although published papers offer several different and sometimes contradictory views on the evolution of the Slavonian Mountains questions about the details of the metamorphic-deformational history, the precise timing of metamorphic events and mineral growth are still open (e.g. *Jamičić*, 1983, 1988; *Pamić*, 1986; *Pamić*

et al., 1988a; *Pamić* and *Lanphere*, 1991 and references therein). The questions arise from the shortcomings of published age data which are either whole-rock data or mineral ages, poorly supported with mineral assemblage descriptions and their relations.

In order to obtain more reliable data on *P–T* conditions and timing of metamorphism we analyzed garnet-bearing micaschist intercalated with gneiss and amphibolite from the Kutjevačka Rijeka transect, which share the same metamorphic evolution (Fig. 1). The samples used in this study are from the same locality preliminary reported by *Balen* and *Horváth* (2003). New mineral and pet-

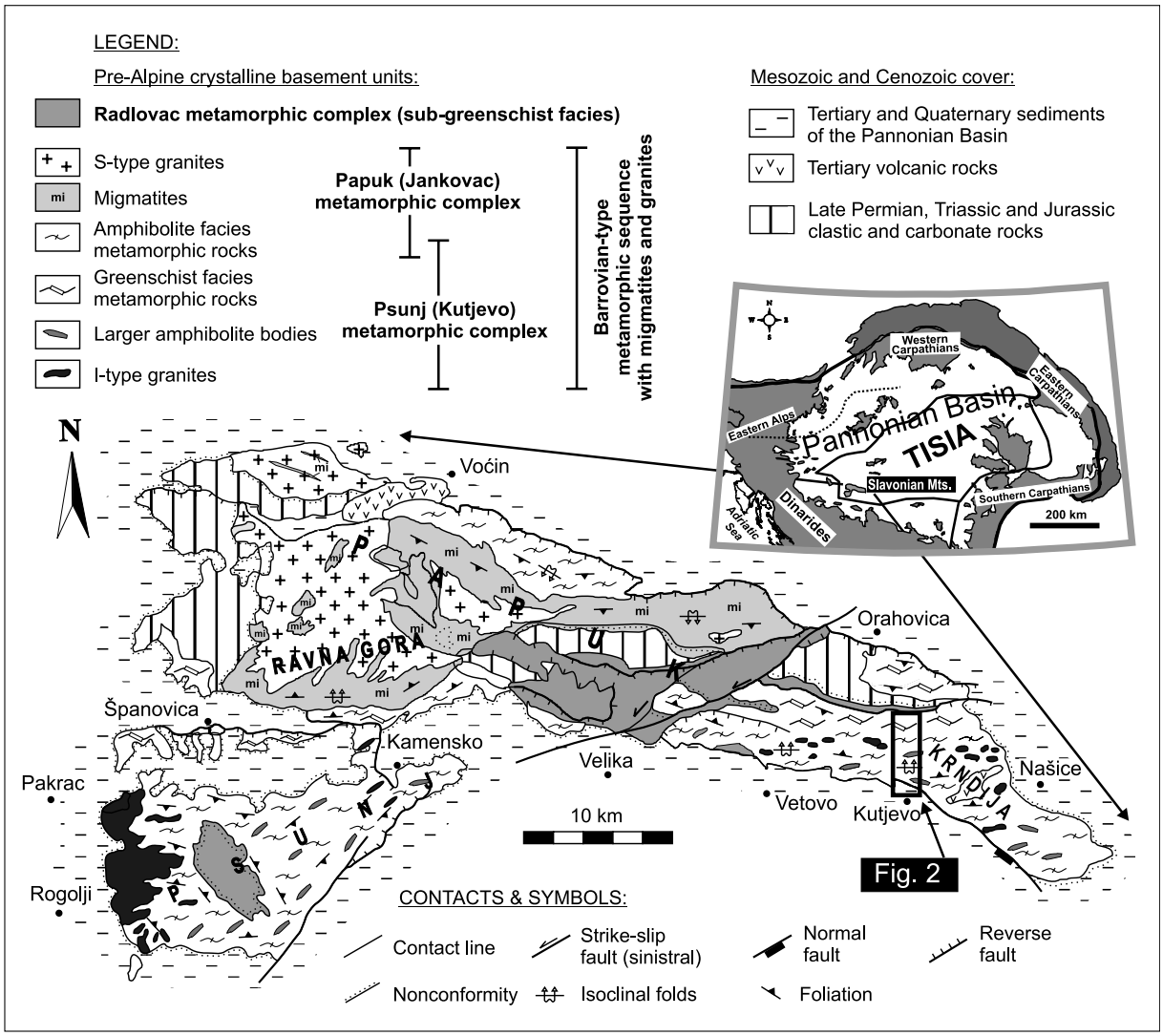

Fig. 1. Simplified geological map of the Slavonian Mts. (after *Jamičić* et al., 1986; *Jamičić* and *Brkić,* 1987; *Jamičić*, 1988; *Pamić* and *Lanphere*, 1991; modified and partly reinterpreted) with inset-map showing the position of the Tisia Unit within the Pannonian Basin. Black-box shows the approximate position of the research area

rological data in combination with meso- to microscopic structural observations and age dating presented here will aid future tectonometamorphic reconstructions and correlations with the European Variscan belt and Paleozoic metamorphic complexes.

The Tisia Unit, which comprises the pre-Neogene basement of the central and southeastern Pannonian Basin (Fig. 1) (e.g. *Csontos*, 1995; *Pamić* et al., 2002) is commonly regarded as a lithospheric fragment broken off from the southern margin of the European plate during the Middle Jurassic (cf. *Géczy*, 1973). It reached its present position after a complex movement history and multiple rotations during Mesozoic and Cenozoic times (e.g. *Csontos*, 1995; *Fodor* et al., 1999; *Csontos* and *Vörös*, 2004). The Slavonian Mts. in northeastern Croatia (Fig. 1) are considered as one of the best exposures of the crystalline basement of the Tisia Unit (e.g. *Pamić* et al., 1996; *Pamić* and *Jurković*, 2002). These rocks experienced a polymetamorphic evolution (*Jamičić*, 1983, 1988) but were most strongly affected by tectono-metamorphic event(s) during the Variscan orogeny (*Pamić* and *Lanphere*, 1991; *Pamić*, 1998; *Haas* et al., 2001; *Pamić* et al., 2002; *Haas* and *Péró*, 2004). Combined geochronological and thermobarometric data obtained from the basement rocks of the Tisia Unit in SE Hungary indicate that these rocks underwent Permian and Eo-Alpine metamorphic overprints (*Árkai* et al., 2000; *Horváth* and *Árkai*, 2002; *Lelkes-Felvári* et al., 2003). Such later overprints have not been documented in the Slavonian Mts.

In this paper we provide new *P–T* data and electron-microprobe age data obtained on monazite grains of garnet-bearing micaschist from the progressively metamorphosed sequence exposed along the Kutjevačka Rijeka transect in the eastern part of the Slavonian Mts. The data presented set new petrological and age constraints for the interpretation of the tectono-metamorphic history of the Tisia Unit.

Geological setting – major pre-Alpine tectonic units and their metamorphic history

The Slavonian Mts. comprise four up to 1000 m high hills called Psunj, Ravna Gora, Papuk and Krndija (Fig. 1). They are located along the southern edge of the Pannonian Basin in northeastern Croatia. In the course of the Neogene to recent tectonic history these hills are seen as a structural assemblage of the pre-Neogene tectonic units, composing a complex WNW–ESE trending positive flower structure formed within a transpressive corridor between the Drava and Sava dextral strike-slip faults (*Jamičić*, 1995). In the central part of the Slavonian Mts. metamorphic and plutonic pre-Alpine rocks are exposed, forming the crystalline basement of the southern part of Tisia Unit (e.g. *Csontos*, 1995; *Pamić* and *Jurković*, 2002; *Pamić* et al., 2002). This crystalline basement is locally covered by Permian-Mesozoic sediments, preserved in cores of map-scale synclines, and predominately by the Neogene-Quaternary fill of the Pannonian Basin (*Jamičić*, 1989; *Jamičić* and *Brkić*, 1987). Later inversions obliterated lithological contacts, which are largely overprinted by younger reverse, normal and strike-slip faults (Fig. 1).

Major tectonic units of the Slavonian Mts.

Jamičić (1983, 1988) distinguished three tectono-metamorphic units (Fig. 1): (1) the Psunj metamorphic complex (also named as the Kutjevo metamorphic series) assumed to be formed by metamorphism during the Baikalian orogeny, overprinted and retrogressed by younger metamorphic events; (2) the Papuk metamorphic complex (also named as the Jankovac metamorphic series), which underwent metamorphism and migmatitization during the Caledonian orogeny, and (3) the Radlovac metamorphic complex which underwent a very low-grade metamorphism during the Variscan orogeny.

The Psunj metamorphic complex consists of (a) greenschist facies metamorphic sequences composed of metapelites, chlorite schists and micaschists, and (b) amphibolite facies metamorphic sequences composed of paragneisses, garnetiferous micaschists, amphibolites, metagabbros and marbles, locally intruded by discordant granodiorites and plagiogranites (i.e. I-type granites according to *Pamić*, 1986; *Pamić* et al., 1988a; *Pamić* and *Lanphere*, 1991).

The Papuk metamorphic complex largely consists of (a) S-type granites (*Pamić*, 1986; *Pamić* et al., 1988a; *Pamić* and *Lanphere*, 1991) surrounded by (b) migmatites and migmatitic gneisses which grade into (c) amphibolite facies metamorphic sequences composed of garnetiferous amphibolites, paragneisses and micaschists.

The Radlovac metamorphic complex consists of very low-grade (sub-greenschist facies) metamorphic sequences largely composed of slates, metagreywackes, metaconglomerates and subordinate phyllites, locally intruded by metadiabases and metagabbros (*Pamić* and *Jamičić*, 1986). According to *Jamičić* (1983, 1988) and *Jamičić* and *Brkić* (1987) this complex occupies the highest structural position in the pre-Alpine complexes from the Slavonian Mts., and originally represents the Late Silurian to Early Permian sedimentary cover over the Psunj (Kutjevo) metamorphic complex (Fig. 1) (*Brkić* et al., 1974; *Jerinić* et al., 1994). It is unconformably covered by a clastic-carbonate succession of Late Permian and Triassic age, which is not affected by Alpine metamorphism (Figs. 1 and 2; *Jamičić* and *Brkić*, 1987).

Based on extensive petrological analysis combined with radiometric age determinations of plutonic and metamorphic rocks *Pamić* and *Lanphere* (1991) put forward an alternative subdivision (Fig. 1) (see also *Pamić* and *Jurković*, 2002 and references therein). They proposed that the Psunj (Kutjevo) and the Papuk (Jankovac) complexes separated by *Jamičić* (1983, 1988) represent a coherent magmatic-metamorphic complex. This complex comprises an E–W trending Barrovian-type metamorphic sequence, which grades continuously into migmatites and granitoids toward the south. The sequence is characterized by the zonal distribution of the index-minerals: chlorite, biotite, almandine, staurolite, sillimanite (*Raffaelli*, 1965), ±kyanite (*Jamičić*, 1983) or andalusite (*Pamić* et al., 1988b). The complex is interpreted to be part of a low-pressure/high temperature metamorphic belt formed during the Variscan orogeny (*Pamić* and *Jurković*, 2002 and references therein) as inferred from geochronological results which include: (1) $^{40}Ar/^{39}Ar$ muscovite plateau ages of paragneisses and micaschists ranging from 333 ± 1.7 to 324.7 ± 1.5 Ma; (2) K–Ar ages for hornblende concentrates from orthoamphibolites ranging from 376.4 ± 11.5 to 352.6 ± 8.5 Ma; (3) Rb/Sr-isochrone ages obtained from whole-rock samples of S-type granites

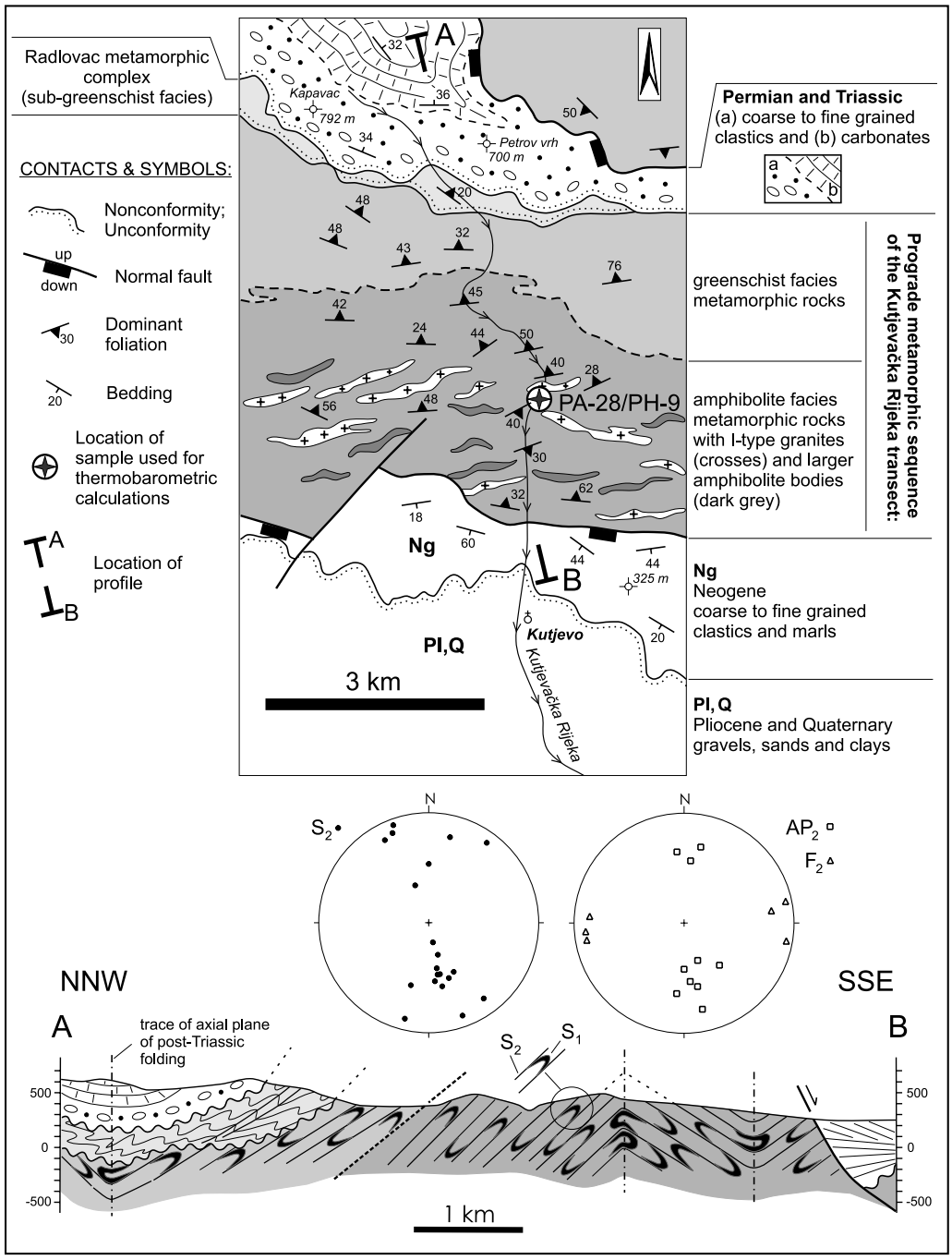

Fig. 2. Geological map in the area of the Kutjevačka Rijeka transect (based on data from *Jamičić* and *Brkić* (1987), partly modified and reinterpreted. Both stereoplots are equal-area, lower hemisphere stereographic representations of D_2 structures in the prograde metamorphic sequence

and migmatites ranging from 314 ± 16 to 317 ± 17 Ma (*Pamić* et al., 1996), and (4) K–Ar muscovite ages from I-type granites ranging from 423.7 ± 12.9 to 336.3 ± 8.4 Ma (*Pamić* et al., 1988a). Besides these, however, *Pamić* et al. (1996)

reported older K–Ar and Ar–Ar muscovite ages around 430 Ma from micaschists of the same complex. These age data provide evidence for a Silurian thermal overprint and give us a hint that the rocks of this area contain pre-Variscan mineral relics. In accordance with the subdivision of *Jamičić* (1983, 1988), they also separated the metadiabase and metagabbro-bearing Radlovac complex, which they interpreted as a very low-grade metamorphic unit of Variscan age.

In spite of the fact that a lot of age dating has been done in the area, a precise age of particular event(s) is still missing. In order to constrain age data and link them to the mineral assemblage we searched for a mineral that provides possibility for *in situ* dating, like monazite.

Analytical methods

Electron microprobe analyses were performed on selected rock samples at the Institute for Geochemical Research, Hungarian Academy of Sciences using a JEOL JCXA-733 electron microprobe equipped with an Oxford INCA 200 EDS. Operating conditions were 20 keV accelerating voltage, 4 nA sample current, and 100 s counting time. The PAP correction procedure was applied (*Pouchou* and *Pichoir*, 1984). The following standards were used: albite for Na, quartz for Si, corundum for Al, MgO for Mg, orthoclase for K, apatite for Ca, hematite for Fe, spessartine for Mn and rutile for Ti.

Monazite dating was carried out at the Salzburg University and follows the procedure described in *Finger* and *Helmy* (1998) with the exception that a maximally focused beam had to be used, owing to the small size of monazite grains. Counting times for the Pb were 180 s on peak and 2^*90 s on background positions, resulting in a 2σ error of ca. 0.013 wt.% for a single point analysis. Counting times for the Th and U were 30 s and 50 s, respectively. Small Y and Th interferences on PbMα were corrected.

Prograde metamorphic sequence along the Kutjevačka Rijeka transect

Mesoscopic observations

Raffaelli (1965) first described a zoned distribution of index minerals within the prograde metamorphic sequence of the Slavonian Mts., west of the N–S striking Kutjevačka Rijeka transect studied here (Figs. 1 and 2). From south to north, the prograde metamorphic sequence is first represented by an amphibolite facies part composed of garnet-bearing micaschist and paragneiss with subordinate orthoamphibolite intercalations and granitoid intrusions (Fig. 2). Further north, greenschists facies schists comprise the low-grade part (chlorite zone) of the metamorphic sequence, which is covered by sub-greenschist facies rocks of the Radlovac metamorphic complex and by a clastic-carbonate Permo-Triassic succession. Mesoscopic observations reveal evidence of two foliations. An older (S_1) foliation is only locally recognized within F_2 fold closures (see structural cross-section of Fig. 2). It represents a metamorphic layering, i.e. a cm-scale alternation of micaschist, paragneiss and amphibolite, which all contain trails of mm-sized garnet grains parallel to the S_1 foliation. This relationship indicates that S_1 formed at

amphibolite facies conditions. Passing from F_2 fold hinges into strongly attenuated limbs, S_1 becomes sub-parallel and parallel to a younger planar fabric (S_2), which is the most evident mesoscopic foliation in these rocks. This foliation is either parallel or shows consistent geometrical relationship with the axial planes (AP_2) of predominantly E–W trending, isoclinal F_2 folds (see stereoplots of Fig. 2). Hence, it is interpreted as to represent an axial plane cleavage of F_2 folds related to the D_2 deformational event, which caused greenschist facies retrogression of the prograde metamorphic sequence. Locally, both S_2 and AP_2 are found to dip in opposite directions, which is interpreted as a result of a subsequent D_3 folding attributed to the Alpine deformation (Fig. 2).

Microscopic observations

Detailed data on mineral assemblages were obtained from the outcrop PA-28/PH-9 (Gauss-Krüger coordinates, X = 6491607, Y = 5033892, 6th zone, Croatia; Fig. 2). This outcrop shows cm-scale alternating layers of micaschist, gneiss and amphibolite (Fig. 3a). Due to ductile deformation, the studied samples are strongly foliated, sporadically showing relicts of microscale isoclinal folds and mylonitic microstructures (Fig. 3b). Mineral assemblage of S_1 foliation corresponds to amphibolite facies (peak metamorphic) conditions while S_2 assemblage corresponds to greenschist facies conditions.

Micaschist has a well preserved metamorphic fabric (S_1) with a peak metamorphic assemblage of garnet, biotite, muscovite, plagioclase and quartz. This foliation is represented by preferentially oriented biotite, muscovite and abundant garnet trails. Plagioclase is elongated, polygonal and round and together with quartz form layers parallel to the S_1. Locally, muscovite forms aggregates with quartz, biotite and garnet. Garnet grains are hypidioblastic, partly fractured, and typically surrounded by asymmetric pressure shadows filled with chlorite, biotite, muscovite, epidote and quartz. Garnets form two distinct groups distinguished by their grain-size. The large-sized garnet population clearly preserves inclusion trails

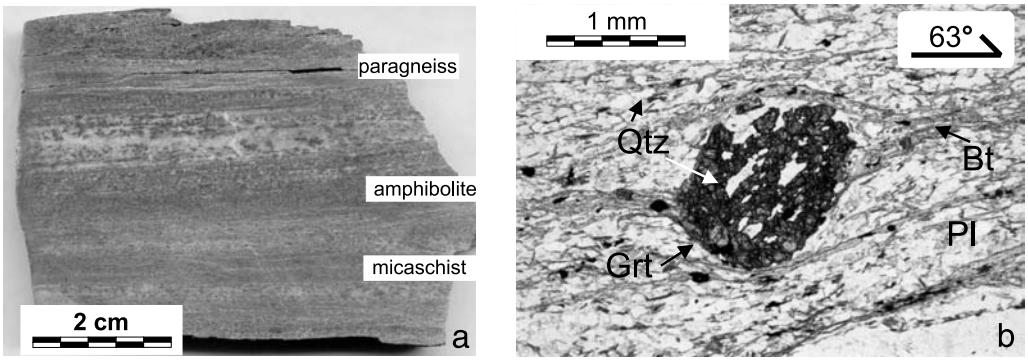

Fig. 3. **a** PA-28/PH-9 sample showing centimeter scale alternating layers of micaschist, paragneiss and amphibolite; **b** Microstructural relations in garnet-bearing micaschist from the Kutjevačka Rijeka transect, plane polarized light, parallel polars, mylonitic microstructure, Bt = biotite, Grt = garnet, Pl = plagioclase, Qtz = quartz

of ilmenite, apatite and quartz, which are aligned oblique to the external foliation (Fig. 3b).

S_2 foliation is related to extensive chloritization of biotite and garnet, pointing to a retrograde process. The formation of the S_2 ductile fabric is therefore interpreted as to represent a deformational event postdating the amphibolite facies metamorphic stage.

The *paragneiss* occurs as thin layers intercalated with micaschist and amphibolite (Fig. 3a). They are well-foliated rocks displaying schistose and gneissose structures defined by elongate mica (biotite) flakes and plagioclase and quartz ribbons. Compared to the micaschist, paragneiss is subordinate and shows a higher modal content of plagioclase and occurrence of amphibole instead of muscovite in the peak assemblage. Together with amphibole the peak assemblage is composed of plagioclase and biotite as dominant phases and garnet (up to $\sim$5 vol.%) and quartz. Biotite is partly chloritized, apatite, zircon and opaques are the accessory minerals.

Nematoblastic garnet-bearing *amphibolite* exhibits lineation and equigranular microstructures. The peak mineral assemblage comprises amphibole with subordinate garnet, plagioclase and quartz. Amphibole is the dominant phase forming prismatic and subheadral grains aligned into lineation. Pleochroism of amphibole is $X' =$ pale yellow, $Y =$ green, and $Z' =$ blue green. Plagioclase occurs as interstitial, xenoblastic grains. Garnets (up to 1 mm) are rounded, pink and looking fresh. Quartz occurs in thin layers and lenses. Accessory minerals are represented by epidote, zoisite, apatite and opaques.

The mineral assemblages of different rock types are shown in Table 1.

Mineral chemistry

The large-sized garnet in the *micaschist* is represented by up to 1 mm-sized subhedral grains which show zonation pattern (Fig. 4a–c). They have Mn-rich

Table 1. *Mineral assemblages of different rock types from the Kutjevačka Rijeka transect*

Rock type	Assemblage		
	I	II (peak)	III
micaschist	core of large garnet grains, accessory minerals (ilmenite, apatite, quartz) in garnet cores	rim of large garnet grains or small garnets, biotite, muscovite, plagioclase, quartz (staurolite?)	muscovite, chlorite, epidote
paragneiss	inclusions in garnet (ilmenite, apatite, quartz, zircon)	garnet, biotite, plagioclase, quartz, hornblende	chlorite, epidote
amphibolite	inclusions in garnet (ilmenite, apatite, epidote, chlorite, plagioclase)	hornblende, plagioclase, garnet, quartz	chlorite, white mica, epidote, zoisite, albite, quartz nests

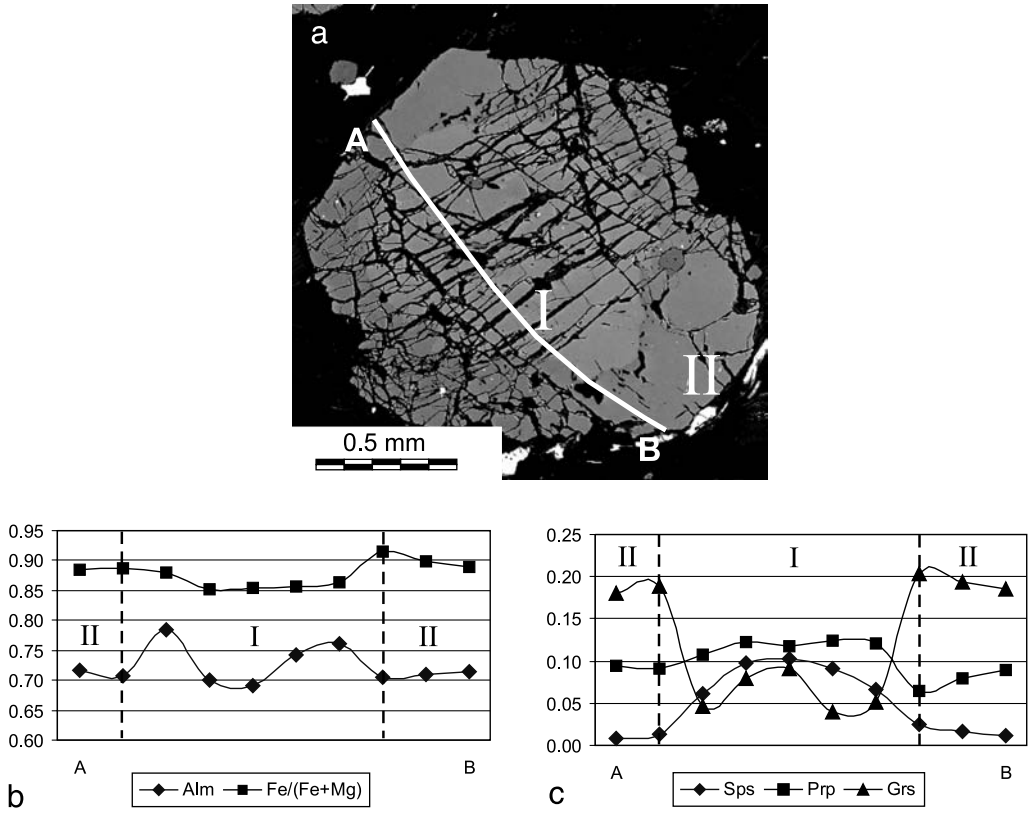

Fig. 4. **a** BSE image of zoned garnet from micaschist, I = core, II = rim; AB line shows position of compositional profile on b and c; **b** Alm = almandine, Fe/(Fe + Mg) ratio; **c** Sps = spessartine, Prp = pyrope, Grs = grossularite + andradite

cores (here referred to as garnet I: $Alm_{68.1}$, $Sps_{10.4}$, $Prp_{12.0}$, $Grs_{7.2}$ and $Adr_{2.2}$) and Ca-rich rims (here referred to as garnet II: $Alm_{70.4–73.1}$, $Sps_{0.6–0.9}$, $Prp_{9.5–9.9}$, $Grs_{13.3–15.1}$ and $Adr_{3.5–3.8}$) – (Table 2). The small-sized garnet grains (up to 0.5 mm in size) have the same chemical composition as observed in the rims of the large garnets (garnet II).

All garnets are almandine rich with smaller amounts of pyrope, grossularite and spessartine components (Table 2). Garnet I usually exhibit higher Mn and Mg and lower Fe and Ca contents than the rim (garnet II). There is an abrupt change in the Ca content between garnets I and II, across a distance of a few micrometers. The small garnets and the rims of large garnets show continuously decreasing X_{Grs}, X_{Sps}, and Fe/(Fe + Mg) ratio and increasing X_{Prp} and X_{Alm} toward garnet rim. Such patterns suggest increasing temperature during the crystallization of garnet rims (*Spear*, 1993). Beside garnet II, peak mineral assemblage comprises biotite, muscovite, plagioclase (17.4–26.3% An) and quartz (Table 2).

The *paragneiss* assemblage comprises garnets with slightly different core ($Alm_{65.1}$, $Sps_{7.9}$, $Prp_{13.2}$, $Grs_{11.3}$ and $Adr_{2.6}$) and rim composition ($Alm_{68.8–70.0}$, $Sps_{4.4–4.6}$, $Prp_{13.8–14.3}$, $Grs_{7.8–9.2}$ and $Adr_{3.5–3.6}$). Peak assemblage includes biotite, calcic amphibole (Si 6.21, Mg 1.95, Fe^{2+} 1.23 p.f.u.) determined as tschermakite following the IMA nomenclature of amphiboles after *Leake* et al. (1997), plagio-

Table 2. *Selected mineral analyses from the micaschist, amphibolite and paragneiss peak mineral assemblages. Cation numbers are calculated on the basis of 12 oxygens for garnet, 22 for micas, 23 for amphibole and 8 for plagioclase. Mineral abbreviations are after* Spear *(1993)*

Micaschist	Garnet				Biotite		Muscovite			Plagioclase	
	core I	rim II	rim II								
SiO_2	37.22	36.36	36.45		35.45	36.03	46.06	45.51		61.07	63.74
TiO_2					1.75	1.74	0.43	0.47			
Al_2O_3	21.29	20.53	20.52		17.84	17.45	36.09	36.03		24.19	22.35
FeO	32.00	33.05	34.06		19.96	20.21	0.93	1.12			
MnO	4.65	0.38	0.28			0.08					
MgO	3.04	2.44	2.34		10.70	10.11	0.26	0.30			
CaO	3.31	6.51	5.78		0.12					5.77	3.66
Na_2O						0.11	2.06	1.45		8.85	9.57
K_2O					8.33	9.37	9.17	10.08		0.15	
Total	101.51	99.27	99.43		94.15	95.10	95.00	94.96		100.03	99.32
Si	2.961	2.956	2.964	Si	5.448	5.518	6.120	6.081	Si	2.718	2.830
Al	1.996	1.967	1.967	Al^{IV}	2.552	2.482	1.880	1.919	Al	1.269	1.169
Fe	2.129	2.247	2.316	Al^{VI}	0.679	0.668	3.771	3.755	Ca	0.275	0.174
Mn	0.313	0.026	0.019	Ti	0.202	0.200	0.043	0.047	Na	0.764	0.824
Mg	0.360	0.296	0.284	Fe	2.565	2.589	0.103	0.125	K	0.009	
Ca	0.282	0.567	0.503	Mn		0.010			Total	5.034	4.997
Total	8.041	8.060	8.053	Mg	2.451	2.308	0.051	0.060			
				Ca	0.020						
Prp	12.0	9.9	9.5	Na		0.033	0.531	0.376	An	26.3	17.4
Sps	10.4	0.9	0.6	K	1.633	1.831	1.554	1.718	Ab	72.9	82.6
Grs	7.2	15.1	13.3	Total	15.550	15.638	14.054	14.081	Or	0.8	
Alm	68.1	70.4	73.1								
Adr	2.2	3.8	3.5	Mg'	48.86	47.13	33.16	32.31			

Paragneiss	Garnet			Biotite		Amphibole		Plagioclase	
	core I	rim II	rim II						
SiO_2	37.81	37.75	37.60		35.41		42.17		60.99
TiO_2					1.78		0.79		
Al_2O_3	20.90	20.73	20.91		17.47		15.25		24.21
FeO	30.64	32.84	33.43		18.43		17.09		
MnO	3.52	2.04	1.97		0.16		0.11		
MgO	3.34	3.50	3.64		11.77		8.88		
CaO	4.92	4.54	3.98				10.71		6.20
Na_2O					0.16		1.56		8.34
K_2O					9.06		0.41		0.04
Total	101.13	101.40	101.53		94.24		96.97		99.78
Si	2.996	2.992	2.978	Si	5.432	Si	6.205	Si	2.718
Al	1.952	1.936	1.952	Al^{IV}	2.568	Al^{IV}	1.795	Al	1.271
Fe	2.031	2.176	2.215	Al^{VI}	0.591	Al^{VI}	0.849	Ca	0.296

(*continued*)

Table 2 (*continued*)

Paragneiss	Garnet				Biotite		Amphibole		Plagioclase
	core I	rim II	rim II						
Mn	0.236	0.137	0.132	Ti	0.205	Ti	0.087	Na	0.720
Mg	0.394	0.413	0.430	Fe	2.364	Fe^{3+}	0.872	K	0.002
Ca	0.418	0.385	0.338	Mn	0.021	Mg	1.947	Total	5.008
Total	8.027	8.040	8.045	Mg	2.691	Fe^{2+}	1.231		
				Na	0.047	Mn	0.014	An	29.1
Prp	13.2	13.8	14.3	K	1.773	Ca	1.688	Ab	70.7
Sps	7.9	4.6	4.4	Total	15.693	Na_{M4}	0.312	Or	0.2
Grs	11.3	9.2	7.8			Na_A	0.133		
Alm	65.1	68.8	70.0	Mg′	53.23	K	0.077		
Adr	2.6	3.6	3.5			Total	15.504		

Amphibolite	Garnet				Amphibole			Plagioclase	
	core I	rim II	rim II						
SiO_2	37.32	36.97	37.11		40.75	46.86		59.92	62.90
TiO_2					0.33	0.53			
Al_2O_3	21.15	20.74	20.51		18.45	10.63		24.99	23.26
FeO	27.62	31.41	31.08		16.49	14.46			
MnO	5.52	2.57	1.95		0.15	0.38			
MgO	2.11	3.18	3.98		7.14	11.53			
CaO	7.35	5.26	4.92		11.82	11.96		6.67	4.83
Na_2O					1.62	0.92		8.11	9.28
K_2O					0.57	0.16		0.24	0.03
Total	101.07	100.13	99.55		97.32	97.43		99.93	100.30
Si	2.969	2.969	2.982	Si	6.068	6.815	Si	2.675	2.778
Al	1.983	1.963	1.942	Al^{IV}	1.932	1.185	Al	1.315	1.211
Fe	1.838	2.109	2.089	Al^{VI}	1.306	0.637	Ca	0.319	0.228
Mn	0.372	0.175	0.133	Ti	0.037	0.058	Na	0.702	0.795
Mg	0.25	0.381	0.477	Fe^{3+}	0.204	0.414	K	0.014	0.002
Ca	0.627	0.452	0.424	Mg	1.585	2.499	Total	5.025	5.014
Total	8.039	8.049	8.046	Fe^{2+}	1.850	1.345			
				Mn	0.018	0.047	An	30.8	22.3
Prp	8.3	12.7	15.9	Ca	1.886	1.864	Ab	67.9	77.5
Sps	12.4	5.8	4.4	Na_{M4}	0.113	0.136	Or	1.3	0.2
Grs	18.5	11.7	10.4	Na_A	0.355	0.123			
Alm	58.4	66.4	65.6	K	0.108	0.030			
Adr	2.4	3.4	3.8	Total	15.530	15.290			

clase (29.1% An) and quartz (Table 2). Apatite, ilmenite, zircon and quartz are inclusions in garnets. Retrograde minerals are the same as in micaschist (chlorite, epidote).

Amphibolite contains garnet with core composition of $Alm_{58.4}$, $Sps_{12.4}$, $Prp_{8.3}$, $Grs_{18.5}$, $Adr_{2.4}$ and rim composition $Alm_{65.6–66.4}$, $Sps_{4.4–5.8}$, $Prp_{12.7–15.9}$, $Grs_{10.4–11.7}$,

$Adr_{3.4-3.8}$. The peak assemblage include calcic amphiboles (Si 6.07–6.82, Mg 1.59–2.50, Fe^{2+} 1.35–1.85 p.f.u.) ranging from subordinate ferrotschermakite to prevailing magnesiohornblende following the IMA nomenclature of amphiboles after *Leake* et al. (1997), plagioclase (22.3–30.8% An) and quartz, with minor ilmenite, apatite, titanite, epidote-clinozoisite (Tables 1 and 2). A relic inclusion assemblage of ilmenite, apatite, epidote, plagioclase and chlorite occur in garnet. Secondary chlorite, muscovite and epidote are present in the studied samples.

Geothermobarometry

Thermobarometric calculations are performed on the peak assemblages (Tables 1 and 2) with garnet II (rims and small-grained garnets) using the average *P–T* method of *Powell* and *Holland* (1988) software THERMOCALC and using the dataset of *Holland* and *Powell* (1990; 1998) as well as individual calibrations of *Graham* and *Powell* (1984) for Grt + Hbl geothermometry, *Holdaway* (2000) for Grt + Bt geothermometry, *Kohn* and *Spear* (1990) for Grt + Hbl + Pl geobarometry and *Holland* and *Blundy* (1994) for Hbl + Pl geothermometry.

For the *micaschist* average *P–T* results range between 600–630 °C and 9–11 kbar using the peak assemblage including Grt II (garnet rim) + Bt + Ms + Pl and Qtz (Table 3).

The peak assemblage Grt rim + Bt + Hbl + Pl + Qtz of *paragneiss* yielded temperature range of 600–620 °C and pressure range between 6.5 and 7.5 kbar (Table 3). Additionally, results for Grt + Hbl + Pl assemblage are at 500–580 °C and 8–10 kbar, 640 °C (Hbl + Pl) and 650 °C (Grt + Bt).

In the *amphibolite* calculated temperature values range between 590 and 620 °C for edenite-richterite and edenite-tremolite reactions, respectively using the geothermometer of *Holland* and *Blundy* (1994). In addition, Grt + Hbl thermometry

Table 3. *Representative results of THERMOCALC v. 3.21 average P–T calculations for the Kutjevačka Rijeka micaschist and paragneiss. End-member and other abbreviations after* Holland *and* Powell *(1990). An expanded file with THERMOCALC output may be obtained on request*

THERMOCALC v. 3.21 Average PT method for garnet rim and coexisting matrix phases	T (°C)	sd	P (kbar)	sd	fit	corr.	aH_2O
Micaschist	633	31	11.0	1.2	0.82	0.800	1.0
	601	36	9.1	1.4	1.28	0.778	1.0
	599	29	8.9	1.1	0.34	0.800	1.0
	607	29	10.6	1.2	0.90	0.776	1.0
	602	28	9.2	1.0	0.57	0.794	1.0
End-members: py, gr, alm, mu, pa, cel, phl, ann, east, an, ab, q, H_2O							
Paragneiss	619	48	7.5	1.4	0.48	0.643	1.0
	603	45	6.7	1.3	0.77	0.650	1.0
End-members: py, gr, alm, phl, ann, east, an, ab, tr, fact, ts, parg, gl, q, H_2O							

yielded temperature of 490–570 °C, and with Grt + Hbl + Pl barometer pressures between 7–10 kbar were obtained.

Monazite dating

In order to constrain the age of the medium grade metamorphism in the Kutjevačka Rijeka transect are used electron-microprobe dating of monazite (*Suzuki* et al., 1991; *Montel* et al., 1996; *Finger* and *Helmy*, 1998). For this purpose several thin sections have been scanned for monazites using the BSE imaging facility. In gneiss samples no monazite was found. However, two micaschists (PA-28/PH-9 and PA-28/PH-9b) contained a few small monazite grains. These occurred in as isolated grains in the matrix and form unusual elongated crystals with ∼2–3 μm width and ∼10–15 μm length. Nineteen such monazites have been analyzed. Results are shown in Table 4.

Table 4. *Electron microprobe analyses of monazites from micaschist samples PA-28/PH-9 and PA-28/PH-9b. Formula units were calculated on the basis of 4 oxygens. Slightly too low totals and cation sums in the A[9] position are due to the fact that Sm, Gd and the HREE were not determined. Model ages were calculated after* Montel *et al. (1996), Th* values after* Suzuki *et al. (1991)*

SAMPLE PA-28/PH-9	m1	m2	m3	m4	m5	m6	m7	m8	m9	m10
SiO_2	0.10	0.17	0.12	0.13	0.13	0.18	0.13	0.07	0.00	0.00
Al_2O_3	0.00	0.02	0.02	0.03	0.01	0.04	0.00	0.00	0.00	0.00
P_2O_5	29.64	29.64	29.71	31.00	31.00	30.32	30.35	30.83	30.08	30.24
CaO	1.16	1.06	1.09	0.95	1.00	1.17	1.10	1.04	1.09	0.96
Y_2O_3	2.31	2.28	2.35	2.82	1.35	2.45	2.62	2.09	2.15	2.61
La_2O_3	11.92	11.96	11.82	12.15	12.71	12.21	12.00	11.83	11.82	12.27
Ce_2O_3	28.98	28.57	28.45	28.31	29.63	27.89	27.93	27.71	27.27	27.38
Pr_2O_3	4.25	4.11	4.09	4.03	4.28	3.92	3.86	3.83	3.77	3.81
Nd_2O_3	13.26	13.32	13.15	12.65	13.11	12.60	13.04	13.30	13.29	12.47
ThO_2	4.01	3.79	4.47	3.30	3.46	3.47	3.25	3.66	4.34	3.11
UO_2	0.85	0.90	0.74	1.09	0.86	1.08	0.96	0.67	0.61	1.10
PbO	0.13	0.12	0.14	0.13	0.12	0.12	0.12	0.11	0.12	0.13
Total	96.62	95.95	96.16	96.58	97.65	95.47	95.37	95.15	94.54	94.09
Si	0.00	0.01	0.00	0.01	0.00	0.01	0.01	0.00	0.00	0.00
P	1.00	1.00	1.01	1.02	1.02	1.02	1.02	1.03	1.02	1.03
Al	0.00	0.00	0.00	0.00	0.00	0.00	0.00	0.00	0.00	0.00
Ca	0.05	0.05	0.05	0.04	0.04	0.05	0.05	0.04	0.05	0.04
Y	0.05	0.05	0.05	0.06	0.03	0.05	0.06	0.04	0.05	0.06
La	0.18	0.18	0.17	0.17	0.18	0.18	0.18	0.17	0.18	0.18
Ce	0.42	0.42	0.42	0.40	0.42	0.40	0.41	0.40	0.40	0.40
Pr	0.06	0.06	0.06	0.06	0.06	0.06	0.06	0.06	0.06	0.06
Nd	0.19	0.19	0.19	0.18	0.18	0.18	0.18	0.19	0.19	0.18
Th	0.04	0.03	0.04	0.03	0.03	0.03	0.03	0.03	0.04	0.03
U	0.01	0.01	0.01	0.01	0.01	0.01	0.01	0.01	0.01	0.01
Pb	0.00	0.00	0.00	0.00	0.00	0.00	0.00	0.00	0.00	0.00

(*continued*)

Table 4 (*continued*)

SAMPLE PA-28/PH-9	m1	m2	m3	m4	m5	m6	m7	m8	m9	m10
Tetr.	1.01	1.01	1.01	1.03	1.03	1.03	1.03	1.04	1.02	1.03
A[9]	0.99	0.98	0.98	0.95	0.96	0.96	0.96	0.94	0.96	0.96
Th	3.523	3.328	3.927	2.901	3.039	3.052	2.856	3.213	3.812	2.734
U	0.753	0.797	0.650	0.962	0.760	0.952	0.843	0.587	0.541	0.970
Pb	0.116	0.111	0.126	0.118	0.113	0.114	0.116	0.102	0.113	0.123
Th*	5.990	5.936	6.062	6.053	5.534	6.166	5.623	5.137	5.588	5.920
Age	**434**	**417**	**464**	**437**	**458**	**413**	**460**	**442**	**453**	**464**
Error	60	60	59	59	65	58	64	70	64	61

SAMPLE PA-28/PH-9b	m1	m2	m3	m4	m5	m6	m7	m8	m9
SiO_2	0.20	0.33	0.16	0.04	0.30	0.35	0.00	0.00	0.00
Al_2O_3	0.07	0.10	0.30	0.01	0.11	0.01	0.00	0.00	0.00
P_2O_5	30.87	30.45	31.28	31.70	30.85	30.62	30.64	30.90	30.68
CaO	1.01	0.85	1.06	0.91	1.28	0.78	1.00	0.97	1.04
Y_2O_3	1.97	1.75	1.84	1.46	1.72	1.45	1.68	1.40	1.49
La_2O_3	13.15	13.36	12.98	13.90	13.11	13.61	13.04	13.96	13.56
Ce_2O_3	30.48	29.41	29.38	30.62	28.97	29.86	30.10	30.31	29.84
Pr_2O_3	4.37	4.13	4.18	4.34	3.98	4.12	4.12	4.35	4.22
Nd_2O_3	12.39	12.77	12.77	12.65	12.74	12.91	12.74	12.53	12.73
ThO_2	3.47	2.94	3.76	2.93	2.60	2.90	3.36	2.69	3.26
UO_2	0.76	0.67	0.76	0.61	0.67	0.60	0.63	0.61	0.70
PbO	0.10	0.10	0.11	0.09	0.08	0.10	0.10	0.09	0.10
Total	98.86	96.87	98.61	99.28	96.42	97.31	97.43	97.81	97.63
Si	0.01	0.01	0.01	0.00	0.01	0.01	0.00	0.00	0.00
P	1.01	1.01	1.02	1.03	1.02	1.01	1.02	1.02	1.02
Al	0.00	0.00	0.01	0.00	0.01	0.00	0.00	0.00	0.00
Ca	0.04	0.04	0.04	0.04	0.05	0.03	0.04	0.04	0.04
Y	0.04	0.04	0.04	0.03	0.04	0.03	0.04	0.03	0.03
La	0.19	0.19	0.18	0.20	0.19	0.20	0.19	0.20	0.20
Ce	0.43	0.42	0.41	0.43	0.41	0.43	0.43	0.43	0.43
Pr	0.06	0.06	0.06	0.06	0.06	0.06	0.06	0.06	0.06
Nd	0.17	0.18	0.18	0.17	0.18	0.18	0.18	0.17	0.18
Th	0.03	0.03	0.03	0.03	0.02	0.03	0.03	0.02	0.03
U	0.01	0.01	0.01	0.01	0.01	0.01	0.01	0.01	0.01
Pb	0.00	0.00	0.00	0.00	0.00	0.00	0.00	0.00	0.00
Tetr.	1.02	1.02	1.02	1.03	1.03	1.03	1.02	1.02	1.02
A[9]	0.97	0.96	0.97	0.96	0.96	0.96	0.97	0.97	0.97
Th	3.052	2.582	3.309	2.579	2.288	2.545	2.955	2.365	2.869
U	0.669	0.595	0.670	0.540	0.587	0.529	0.559	0.539	0.620
Pb	0.095	0.089	0.101	0.088	0.075	0.090	0.093	0.081	0.092
Th*	5.240	4.532	5.500	4.350	4.207	4.284	4.787	4.131	4.901
Age	**407**	**439**	**411**	**452**	**398**	**470**	**436**	**441**	**422**
Error	68	79	65	82	85	84	75	87	73

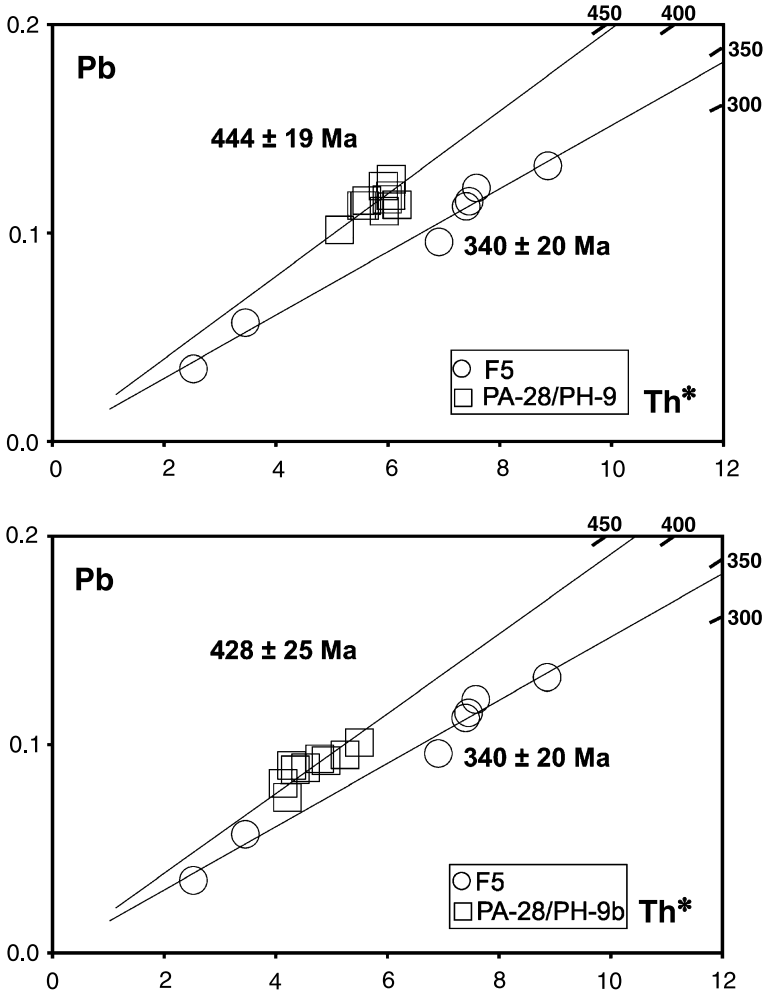

Fig. 5. Total Pb vs. Th^* isochron diagrams after *Suzuki* et al. (1991) for the monazites from samples PA-28/PH-9 and PA-28/PH-9b (see Table 4). A monazite age standard (F_5) has been measured for control, the recommended age of 341 Ma could be reproduced. Time scale shown is based on the position of zero-intersect isochrons. Drawn isochrons refer to the calculated weighted average ages for sample and standard monazites

The measured Th–U–Pb concentrations indicate that these monazites were formed during the Ordovician-Silurian. The single point ages calculated after *Montel* et al. (1996) are all consistent within error and cluster around weighted averages of 444 ± 19 and 428 ± 25 Ma in the two samples (Fig. 5). There is no evidence for a polygenetic nature of the monazite populations. The most plausible interpretation is that the obtained average ages of 444 ± 19 and 428 ± 25 Ma date the medium-grade metamorphism in these rocks. This interpretation is additionally supported by the partly very high yttrium contents of the monazites (almost 3 wt.% Y_2O_3). Such high yttrium contents are indicative of monazite growth at middle or upper amphibolite facies conditions (*Spear* and *Pyle*, 2002), and thus in agreement with the *P–T* estimates derived for the host rocks by means of geothermometry (see above).

Discussion

P–T calculations were carried out using compositions of coexisting mineral assemblages, assumed to represent equilibrium conditions. THERMOCALC average temperature estimations are strongly dependent on composition of minerals which in analyzed rocks may not be in equilibrium state or are partly re-equilibrated during the retrograde evolution. Therefore, note that the *P–T* calculations given above should be regarded as range data which include all mineral chemical composition variations inside assemblages.

Obtained peak *P–T* data are in good agreement with expected values for observed assemblages but represent only one fixed point during the *P–T* evolution. Prior to peak conditions initial garnet growth started at upper greenschist or lower amphibolite facies conditions as deduced from epidote and chlorite inclusions in the garnets from intercalated amphibolite. The garnet rim achieved equilibrium with matrix minerals at the peak metamorphic conditions in range of 600–650 °C and 8–11 kbar.

Monazite ages of 444 ± 19 and 428 ± 25 Ma obtained in our study indicate that the medium-grade metamorphism recorded in micaschist from the Kutjevačka Rijeka transect is related to a tectonothermal event in the Early Paleozoic (Ordovician to Silurian following the geologic time scale of *Gradstein* et al., 2004) – thus it is related to the pre-Variscan event.

The correlation of Th–U–Pb monazite age data with specific thermal and deformational event in metamorphic rocks may be problematic (*Williams* and *Jercinovic*, 2002) since monazite occurs as small accessory grains that do not define tectonic foliations and hence are difficult to link directly to particular metamorphic assemblage or tectonic fabric. Although, there is no unequivocal evidence that the monazite belongs to the peak *P–T* mineral assemblage, this can be considered likely due to the high Y content of monazite which links monazite with the medium to grade metamorphism and S_1 foliation.

As shown by mesoscopic to microscopic observations, the formation of S_2 fabric indicates that the later overprint occurred at greenschist facies conditions that predates the Alpine deformation. However, due to the lack of minerals suitable for radiometric dating, it is not quite clear whether the S_2 fabric formed during cooling from a single pre-Variscan clockwise *P–T* evolution or if it marks a subsequent metamorphic event related to Variscan orogeny as may be suggested by numerous Variscan ages summarized by *Pamić* and *Jurković* (2002).

The presented peak metamorphic data together with additional microstructural, paragenetic, mineral chemical and age data cannot be directly correlated with results and available *P–T* path reconstructions obtained in the nearby parts of the Tisia in Hungary (e.g. *Árkai* et al., 1999; *Horváth* and *Árkai*, 2002). No isotopic ages older than Variscan are available from the metamorphic basement of the Tisia Unit in Hungary (*Lelkes-Felvári* et al., 1996). Furthermore, available data for the eventual analogues from the Alps (*Neubauer* et al., 1999, 2003; *Schaltegger* et al., 2003) are too scarce to be used for a reliable geodynamic interpretation.

Future work in the area will be confronted with the challenge to separate pre-Variscan and Variscan metamorphism on a regional scale, to derive *P–T* data and

metamorphic isograds for both events separately, and to set unequivocal relationships between magmatic and metamorphic rocks and events.

Conclusions

1. Peak metamorphic conditions for micaschist, paragneiss and amphibolite from the Kutjevačka Rijeka transect are in the ranges of ca. 600–650 °C and 8–11 kbar and correspond to amphibolite facies conditions.
2. Obtained Th–U–Pb ages of 444 ± 19 and 428 ± 25 Ma for monazite grains from garnet-bearing micaschist indicate a pre-Variscan event (Ordovician-Silurian) and are attributed to the particular tectonometamorphic event which resulted in formation of S_1 foliation and the peak metamorphic assemblage.
3. The medium-grade metamorphic rocks were subsequently overprinted by a retrograde greenschist facies metamorphic event marked by younger (S_2) planar fabric. Development of S_2 fabric predates the Alpine deformation, hence it is tentatively attributed to the Variscan orogeny.

Acknowledgements

The authors wish to express their gratitude to the late Professor Jakob Pamić who started and encouraged this research in the frame of project "Comparative metamorphic petrogenetic study of Internal Dinarides, Bükk Unit and Tisia". We have lost not only an outstanding scientist, but also a gentleman and a friend. This project has been elaborated within the frame of bilateral agreement held between the Croatian Academy of Sciences and Arts and the Hungarian Academy of Sciences. This study was also financially supported by the current projects of Ministry of Science, Education and Sports of the Republic of Croatia (DB and BT) and the Hungarian National Science Fund (OTKA) project no. F 047322 (PH). Critical reviews and comments by *A. Zeh*, an anonymous referee and associate editor *K. Stüwe* greatly improved the manuscript.

References

Árkai P, Horváth P, Nagy G (1999) A clockwise P–T path from the Variscan basement of the Tisza Unit, Pannonian Basin, Hungary. Geol Croatica 52: 109–117

Árkai P, Bérczi-Makk A, Balogh K (2000) Alpine low-T prograde metamorphism in the post-Variscan basement of the Great Plain, Tisza Unit (Pannonian Basin, Hungary). Acta Geol Hungarica 43: 43–63

Balen D, Horváth P (2003) The geothermobarometry of Variscan medium-grade metamorphic rocks from the Kutjevačka Rijeka (Slavonian Mts., Croatia). J Czech Geol Soc 48: 17–18

Brkić M, Jamičić D, Pantić N (1974) Karbonske naslage u Papuku (sjeveroistočna Hrvatska) (Carboniferous deposits in Mount Papuk (northeastern Croatia)). Geol vjesnik Zagreb 27: 53–58 (in Croatian)

Csontos L (1995) Tertiary tectonic evolution of the Intra-Carpathian area: a review. Acta Vulcanol 7: 1–13

Csontos L, Vörös A (2004) Mesozoic plate tectonic reconstruction of the Carpathian region. Palaeogeogr Palaeoecl 210: 1–56

Finger F, Helmy HM (1998) Composition and total-Pb model ages of monazites from high-grade paragneisses in the Abu Swayel area, southern Eastern Desert, Egypt. Mineral Petrol 62: 269–289

Fodor L, Csontos L, Bada G, Györfi I, Benkovics L (1999) Tertiary tectonic evolution of the Pannonian Basin system and neighbouring orogens: a new synthesis of palaeostress data. In: *Durand D, Jolivet L, Horváth F, Séranne M* (eds) The Mediterranean basins: Tertiary extension within the Alpine orogen. Geol Soc Spec Publ 156: 295–334

Géczy B (1973) The origin of the Jurassic faunal provinces and the Mediterranean plate tectonics. Ann Univ Sci Budapest, Eötvös Nom Sect Geol 16: 99–114

Gradstein F, Ogg JG, Smith AGM, Agterberg FP, Bleeker W, Cooper RA, Davydov V, Gibbard P, Hinnov LA, House MR, Lourens L, Luterbacher HP, McArthur J, Melchin MJ, Robb LJ, Shergold J, Villeneuve M, Wardlaw BR, Ali J, Brinkhuis H, Hilgen FJ, Hooker J, Howarth RJ, Knoll AH, Laskar J, Monechi S, Plumb KA, Powell J, Raffi I, Röhl U, Sadler P, Sanfilippo A, Schmitz B, Shackleton NJ, Shields GA, Strauss H, van Dam J, van Kolfschoten T, Veizer J, Wilson D (2004) A geologic time scale. Cambridge University Press, Cambridge

Graham CM, Powell R (1984) A garnet-hornblende geothermometer: calibration, testing and application to the Pelona Schists, Southern California. J Metamorph Geol 2: 13–34

Haas J, Péró C (2004) Mesozoic evolution of the Tisza Mega-unit. Int J Earth Sci 93: 297–313

Haas J, Hámor G, Jámbor Á, Kovács S, Nagymarosy A, Szederkényi T (2001) Geology of Hungary. Eötvös University press, Budapest

Holdaway MJ (2000) Application of new experimental and garnet Margules data to the garnet-biotite geothermometer. Am Mineral 85: 881–892

Holland TJB, Blundy J (1994) Non-ideal interactions in calcic amphiboles and their bearing on amphibole-plagioclase thermometry. Contrib Mineral Petrol 116: 433–447

Holland TJB, Powell R (1990) An enlarged and updated internally consistent thermodynamic dataset with uncertainties and correlations: the system K_2O–Na_2O–CaO–MgO–MnO–FeO–Fe_2O_3–Al_2O_3–TiO_2–SiO_2–C–H_2–O_2. J Metamorph Geol 8: 89–124

Holland TJB, Powell R (1998) An internally consistent thermodynamic dataset for phases of petrological interest. J Metamorph Geol 16: 309–343

Horváth P, Árkai P (2002) Pressure-temperature path of metapelites from the Algyö-Ferencszállás area, SE Hungary: thermobarometric constraints from coexisting mineral assemblages and garnet zoning. Acta Geol Hungarica 45: 1–27

Jamičić D (1983) Strukturni sklop metamorfnih stijena Krndije i južnih padina Papuka (Structural fabric of the metamorphosed rocks of Mt. Krndija and the eastern part of Mt. Papuk). Geol vjesnik Zagreb 36: 51–72 (in Croatian)

Jamičić D (1988) Strukturni sklop slavonskih planina (Tectonics of the Slavonian Mts.). PhD Thesis, University of Zagreb, pp 152 (in Croatian)

Jamičić D (1995) The role of sinistral strike-slip faults in the formation of the structural fabric of the Slavonian Mts. (Eastern Croatia). Geol Croatica 48: 155–160

Jamičić D (1989) Basic geological map of Yugoslavia in scale 1:100.000, sheet Daruvar. Geol Inst Zagreb, Fed Geol Inst Beograd

Jamičić D, Brkić M (1987) Basic geological map of Yugoslavia in scale 1:100.000, sheet Orahovica. Geol Inst Zagreb, Fed Geol Inst Beograd

Jamičić D, Brkić M, Crnko J, Vragović M (1986) Basic geological map of Yugoslavia – Explanatory notes for sheet Orahovica. Geol Inst Zagreb, Fed Geol Inst Beograd

Jerinić G, Pamić J, Sremac J, Španić D (1994) First palynological data and organic-petrographic data on very low- and low-grade metamorphic rocks in Slavonian Mountains (North Croatia). Geol Croatica 47: 149–155

Kohn MJ, Spear FS (1990) Two new geobarometers for garnet amphibolites, with applications to southeastern Vermont. Am Mineral 75: 89–96

Leake BE, Woolley AR, Arps CES, Birch WD, Gilbert MC, Grice JD, Hawthorne FC, Kato A, Kisch HJ, Krivovichev VG, Linthout K, Laird J, Mandarino J, Maresch WV, Nickel EH, Rock NMS, Schumacher JC, Smith DC, Stephenson NCN, Ungaretti L, Whitaker EJW, Youzhi G (1997) Nomenclature of amphiboles: Report of the Subcommittee on amphiboles of the International Mineralogical Association, Commission on New Minerals and Mineral Names. Can Mineral 35: 219–246

Lelkes-Felvári Gy, Árkai P, Sassi FP, Balogh K (1996) Main features of the regional metamorphic events in Hungary: a review. Geol Carpathica 47: 257–270

Lelkes-Felvári Gy, Frank W, Schuster R (2003) Geochronological constraints of the Variscan, Permian-Triassic and eo-Alpine (Cretaceous) evolution of the Great Hungarian Plain basement. Geol Carpathica 54: 299–315

Montel JM, Foret S, Veschambre M, Nicollet C, Provost A (1996) Electron microprobe dating of monazite. Chem Geol 131: 37–53

Neubauer F, Hoinkes G, Sassi FP, Handler R, Höck V, Koller F, Frank W (1999) Pre-Alpine metamorphism of the Eastern Alps. Schweiz Mineral Petrogr Mitt 79: 41–62

Neubauer F, Frisch W, Hansen BT (2003) Early Paleozoic and Variscan events in the Austroalpine Rennfeld block (Eastern Alps): A U–Pb study. Jb Geol B–A 143: 567–580

Pamić J (1986) Magmatic and metamorphic complexes of the adjoining area of the northernmost Dinarides and Pannonian Mass. Acta Geol Hungarica 29: 203–220

Pamić J (1998) Crystalline basement of the South Pannonian Basin based on surface and subsurface data. Nafta Zagreb 49: 371–390

Pamić J, Jamičić D (1986) Metabasic intrusive rocks from the Paleozoic Radlovac complex of Mt. Papuk in Slavonija (northern Croatia). Rad Jugosl Akad Znan Umjet Zagreb 424: 97–125

Pamić J, Jurković I (2002) Paleozoic tectonostratigraphic units in the northwest and central Dinarides and the adjoining South Tisia. Int J Earth Sci 91: 538–554

Pamić J, Lanphere M (1991) Hercynian granites and metamorphic rocks from the Papuk, Psunj, Krndija and the surrounding basement of the Pannonian Basin (Northern Croatia, Yugoslavia). Geologija Ljubljana 34: 81–253

Pamić J, Lanphere M, McKee E (1988a) Radiometric ages of metamorphic and associated igneous rocks of the Slavonian Mountains in the southern part of the Pannonian Basin, Yugoslavia. Acta Geol Zagreb 18: 13–39

Pamić J, Lelkes-Felvári Gy, Raffaelli P (1988b) Andalusite-bearing schists from the southwestern parts of Papuk Mt. in Slavonija (northern Croatia). Geol vjesnik Zagreb 41: 145–157

Pamić J, Lanphere M, Belak M (1996) Hercynian I-type and and S-type granitoids from the Slavonian Mountains (southern Pannonian, north Croatia). N Jb Mineral Abh 171: 155–186

Pamić J, Balen D, Tibljaš D (2002) Petrology and geochemistry of orthoamphibolites from the Variscan metamorphic sequences of the South Tisia in Croatia – an overview with geodynamic implications. Int J Earth Sci 91: 787–798

Pouchou JL, Pichoir F (1984) A new model for quantitative X-ray microanalyses, Part I. Application to the analyses of homogenous samples. Recherche Aerospatiale 3: 13–38

Powell R, Holland TJB (1988) An internally consistent dataset with uncertainties and correlations: 3. Applications to geobarometry, worked examples and a computer program. J Metamorph Geol 6: 173–204

Raffaelli P (1965) Metamorphism of Paleozoic pelitic schists of Ravna Gora (Papuk Mountain – Croatia). Geol vjesnik Zagreb 18: 61–111 (in Croatian)

Schaltegger U, Abrecht J, Corfu F (2003) The Ordovician orogeny in the Alpine basement: constraints from geochronology and geochemistry in the Aar Massif (Central Alps). Schweiz Mineral Petrogr Mitt 83: 183–195

Spear FS (1993) Metamorphic phase equilibria and pressure-temperature-time paths. Mineral Soc Am Monograph, BookCrafters, Washington DC

Spear FS, Pyle JM (2002) Apatite, monazite and xenotime in metamorphic rocks. In: *Kohn MJ, Rakovan J, Hughes JM* (eds) Phosphates: geochemical, geobiological and materials importance. Mineral Soc Am Rev Mineral 48: 293–336

Suzuki K, Adachi M, Tanaka T (1991) Middle Precambrian provenance of Jurassic sandstone in the Mino Terrane, central Japan: Th–U–total Pb evidence from an electron microprobe monazite study. Sed Geol 75: 141–147

Williams ML, Jercinovic MJ (2002) Microprobe monazite geochronology: putting absolute time into microstructural analysis. J Struct Geol 24: 1013–1028

Authors' addresses: *D. Balen* (corresponding author; e-mail: drbalen@geol.pmf.hr), Faculty of Science, University of Zagreb, Horvatovac bb, HR-10000 Zagreb, Croatia; *P. Horváth*, *P. Árkai*, Institute for Geochemical Research, Hungarian Academy of Sciences, Budaörsi út 45, H-1112 Budapest, Hungary; *B. Tomljenović*, Faculty of Mining, Geology & Petroleum Engineering, University of Zagreb, Pierottijeva 6, HR-10000 Zagreb, Croatia; *F. Finger*, *B. Humer*, Abteilung Mineralogie und Materialwissenschaften, Universität Salzburg, Helbrunnerstrasse 34, A-5020 Salzburg, Austria